Using Nanotechnology to Control Oxidant Levels

Undergraduate Honors Thesis

Department of Cell and Molecular Biology

Alexandra Meilhac

April 1st, 2017

Table of Contents

Acknowledgments

I would like to thank Dr. Howard Petty and Andrea Clark for their mentorship and continued support.

Abstract

Several current cancer therapies, including photodynamic therapy (PDT), use reactive oxygen species (ROS) to induce tumor cell apoptosis and necrosis. Photocatalytic tungsten trioxide platinum (WO_3/Pt) nanoparticles constitute a novel therapeutic agent for promoting hydroxyl radical production during PDT. In the present study, we develop a targetable and chemically active form of WO_3/Pt nanoparticles for applications in cancer treatment. Orthorhombic WO_3 nanoparticles platinized at basic pH were used due to their exceptional catalytic activity under visible light illumination. When modified with tumor specific amino ligands for targeted delivery, these nanoparticles continued to express tumor toxicity via ROS production. The ability to use targetable inorganic nanoparticles for PDT may contribute to eventually improving patient outcomes.

Introduction

Nanoparticles are ideally sized to interact with cell surfaces and biological systems at the molecular level. For this reason, they have been tailored with targeting peptides to function as drug delivery systems. For example, gold nanoparticles conjugated with tumor necrosis factor and paclitaxel, a tumor targeting moiety and an anticancer drug, cause tumor regression in mice.[8] However, metal oxide nanoparticles may also function as therapeutic agents because of their radical scavenging and anticancer properties. By catalyzing redox reactions, metal oxide nanoparticles can transfer electrons between species, creating or detoxifying reactive oxygen species (ROS). ROS are responsible for a number of diseases including cardiovascular and neurodegenerative diseases. While excessive ROS can induce oxidative stress and cause significant cell damage, basal levels of ROS are also necessary for cellular homeostasis.[7] Therefore, metal oxide nanoparticles are suitable candidates for exogenously controlling ROS levels. Here, we explore using photocatalytic WO_3/Pt nanoparticles to elevate ROS levels in tumor cells for improved cancer treatment.

WO_3 are photocatalytic nanoparticles that generate hydroxyl radicals when stimulated with visible light. Hydroxyl radicals are a reactive oxygen species that can cause significant damage to intracellular molecules and induce cell apoptosis and necrosis.[9] When loaded with platinum, WO_3 nanoparticles demonstrate enhanced photocatalytic activity and increased ROS production.[1] Thus, WO_3/Pt nanoparticles may be used to promote ROS-induced tumor cell death.

Current cancer treatments that rely on ROS to eradicate tumor cells are suboptimal. In photodynamic therapy (PDT), photosensitizer dyes accumulate in tumor tissue and generate reactive oxygen species (ROS) upon exposure to light. However, traditional first and second generation photosensitizers are hydrophobic and show poor tumor selectivity.[2,9] Moreover, they

are also readily degraded by ROS produced during illumination. As a result, photosensitizers limit the duration of therapy since their half-lives typically lie on the order of minutes to hours.

WO_3/Pt photocatalytic nanoparticles offer a critical advantage for improving PDT in cancer patients. For one, WO_3/Pt nanoparticles do not photobleach due to their inorganic nature, allowing for increased ROS yields over time. This could potentially improve patient outcomes by prolonging the treatment period. For another, WO_3/Pt nanoparticles can be functionalized to target tumor cells through surface modifications. Indeed, the surface chemistry of WO_3/Pt enables conjugation of tumor specific amino ligands, such as folic acid. Folic acid binds folate receptor which is overexpressed in cancer cells.[6] Therefore, active targeting of WO_3/Pt nanoparticles could increase selectivity relative to photosensitizers. Finally, WO_3/Pt nanoparticles have X-ray scattering properties that could be used to track nanoparticle movements in patients using micro-CT scans.

Among semiconductors, WO_3/Pt nanoparticles are ideal candidates for PDT. For one, their band gap is small enough for visible-light activation (2.4–2.8 eV).[11] By contrast, UV light-activated semiconductors such as TiO_2 are unfit for PDT since UV radiation causes DNA damage. For another, WO_3/Pt nanoparticles demonstrate high efficiency for decomposition of organic compounds due to the high oxidation power of their valence band holes.[11] This suggests that WO_3/Pt nanoparticles would be active photocatalysts in a biological environment.

Importantly, WO_3 is nontoxic and has exceptional stability in aqueous media over a wide pH range.[7] Moreover, the median lethal dose of WO_3 (1059 mg/kg) is greater than that of caffeine (150-200 mg), suggesting that WO_3 nanoparticles are safe to use in appropriate doses.[10] Although the toxicity of WO_3/Pt nanoparticles has not been established, recent studies indicate that WO_3/Pt nanoparticles have no effect on ocular structures when injected into the anterior chamber of a mouse eye.[10]

Taken together, WO_3/Pt nanoparticles may serve as an alternative to current photosensitizers for treatment of cancer using PDT. Interestingly, the literature on WO_3/Pt nanoparticles has focused on environmental solutions, and the biomedical applications of WO_3/Pt photocatalysts remain unexplored.[5] With a view toward developing nanotherapeutics, we have performed experiments testing the anticancer properties of WO_3/Pt.

Materials and Methods

Photoanode activity

We assessed the photoanode activity of WO_3/Pt nanoparticles by monitoring the degradation of methylene blue over time. A suspension of 0.5 mg/mL of WO_3/Pt nanoparticles in 46.9 mM methylene blue was illuminated with a visible light source. Aliquots were taken at time intervals and centrifuged to remove nanoparticles. Supernatants were transferred to Costar plates and absorbance was read at 660 nm with a plate reader (Molecular Devices).

Photocathode activity

We assessed the photocathode activity of WO_3/Pt nanoparticles by using coumarin as a fluorescent probe to monitor hydroxyl radical production. Hydroxyl radicals react with coumarin to form a fluorescent compound. A suspension of 0.5 mg/mL of WO_3/Pt nanoparticles in 1mM coumarin (pH 3) was illuminated with a visible light source for ninety minutes. Aliquots were sampled at eight different time points and centrifuged to remove nanoparticles. Supernatants were transferred to Costar plates and read with a FlexStation II device (Molecular Devices) with excitation at 332 nm emission at 460 nm.

Dissolved oxygen measurements

We assessed the ability of a panel of biomolecules to act as substrates for WO_3/Pt nanoparticles by monitoring oxygen utilization. A suspension of 1 mg/mL of WO_3/Pt nanoparticles in 1mM lysine was illuminated with a visible light source in customized Hach (Loveland, CO) BOD bottles at room temperature. Dissolved oxygen was measured using an Oakton model DO2700 meter (Cole-Parmer, Vernon Hills, IL) with constant stirring. Arginine, glucose, glycerol, citric acid, oxalic acid and uridine were also tested as substrates for the catalysis of hydroxyl radicals from oxygen by WO_3/Pt nanoparticles.

Gel electrophoresis

We confirmed the conjugation of FA-PEG to WO_3/Pt nanoparticles using gel electrophoresis to assess nanoparticle electro-kinetic properties. 25 µg of WO_3/Pt nanoparticles were loaded per well in a 0.4% agarose gel submerged in 1x TAE buffer. Electrophoresis was run at 60 mA for one hour.

Antibody staining

We confirmed the conjugation of FA-PEG to WO_3/Pt nanoparticles using antibody staining. FA-PEG WO_3/Pt nanoparticles in 1% BSA were stained with mouse anti folic acid antibody in a 1:50 dilution. After sixty minutes, nanoparticles were washed three times with PBS and subsequently stained with Alexa Fluoro Goat anti mouse antibody in a 1:50 dilution. Nanoparticles were visualized using immunofluorescence microscopy.

Statistical Analysis

In vitro data are presented as the mean ± standard deviation. Data were evaluated with Student's t-test.

Results

Crystal structure and platinization pH affect WO_3/Pt catalytic activity.

We evaluated the effect of crystal structure and platinization pH on WO_3/Pt catalytic activity. Nanoparticles platinized at acidic (pH = 2) and basic (pH = 12) pH were illuminated with light in the presence of coumarin for 30 minutes. Fluorescence was measured over time to monitor the production of hydroxyl radicals (332/460). At 30 minutes, WO_3/Pt nanoparticles platinized at basic pH generated significantly more hydroxyl radicals than WO_3/Pt nanoparticles platinized at acidic pH ($p = 0.001$). Next, we tested the catalytic activity of orthorhombic and tetragonal nanoparticles. After 30 minutes of illumination, orthorhombic nanoparticles incubated with coumarin produced significantly more hydroxyl radicals than tetragonal nanoparticles ($p = 0.02$). In the absence of nanoparticles, hydroxyl radicals were not produced (data not shown).

WO_3/Pt nanoparticles use light to degrade organic dyes.

We evaluated the ability for WO_3/Pt nanoparticles to degrade organic dyes under visible light illumination. We illuminated WO_3/Pt nanoparticles with methylene blue, which has a peak absorbance at 660 nm. Degradation of methylene blue was evaluated using spectrophotometry. When illuminated in the presence of nanoparticles, methylene blue disappears over time (Figure 4). In the absence of light or nanoparticles, methylene blue is not degraded (data not shown).

Biological molecules are substrates for WO_3/Pt nanoparticles.

We conducted oxygen utilization experiments to study the substrate specificity of WO_3/Pt nanoparticles. Among the biomolecules tested were glucose, lysine, uridine, citric acid, and arginine. To determine if biomolecules are substrates for WO_3/Pt nanoparticles, we incubated them with nanoparticles under illumination. In the absence of substrate, illuminated nanoparticles do not consume oxygen (Figure 5, Trace 1). Similarly, in the absence of nanoparticles, the substrate lysine does not diminish oxygen levels (Figure 5, Trace 2). In the

dark, nanoparticles incubated with lysine do not consume oxygen (Figure 5, Trace 3). However, when nanoparticles are incubated with lysine under visible light illumination, oxygen is depleted (Figure 5, Trace 4). Thus, lysine is a substrate for WO_3/Pt nanoparticles. Similarly, glucose, lysine, uridine, citric acid, and arginine promote oxygen disappearance during nanoparticle illumination (Figure 5, Traces 5-10) suggesting that a large panel of biomolecules including amino acids, metabolites, and nucleosides are substrates for WO_3/Pt nanoparticles.

WO_3/Pt nanoparticles are surface modified with tumor targeting peptides using CDI.

We functionalized WO_3/Pt nanoparticles with folic acid, a tumor specific amino ligand. First, WO_3/Pt nanoparticles were activated with carbonyldiimidazole (CDI). Then, WO_3/Pt nanoparticles were reacted with FA-PEG-NH_2 to form FA-PEG WO_3/Pt nanoparticles (Figure 6A). Polyethylene glycol was used to stabilize nanoparticle suspensions and prevent aggregation. To confirm the linkage of folic acid to nanoparticles, we electrophoresed modified and unmodified nanoparticles on a 0.4% agarose gel. FA-PEG coated nanoparticles migrated a shorter distance than unmodified nanoparticles, suggesting that FA-PEG alters the electro-kinetic properties of WO_3/Pt nanoparticles (Figure 6C). Moreover, we also stained nanoparticles with mouse anti folic acid antibody and Alexa Fluor 488 goat anti mouse antibody. Under microscope, FA-PEG coated nanoparticles fluoresced (Figure 6B) whereas unmodified nanoparticles did not (data not shown). These results confirm that CDI effectively conjugates FA-PEG to WO_3/Pt nanoparticles. In subsequent conjugations, CDI was used to link PLL and PVA to WO_3/Pt nanoparticles. After conjugation, FA-NHS ester was reacted with amino groups on PLL and PVA to form FA-PLL and FA-PVA WO_3/Pt nanoparticles. We confirmed the presence of FA on FA-PLL and FA-PVA WO_3/Pt nanoparticles using immunofluorescence (data not shown).

Surface-modified WO_3/Pt nanoparticles remain chemically active.

We tested the catalytic activity of FA-PEG, FA-PLL, and FA-PVA WO_3/Pt nanoparticles by monitoring the production of hydroxyl radicals using coumarin as a fluorescent probe. Nanoparticles were illuminated with coumarin for 90 minutes. Aliquots were sampled at eight different time points and assessed for fluorescence (332/460). Catalytic activity of nanoparticles was measured before and after surface modification. We found that FA-PEG and FA-PLL nanoparticles retain their ability to synthesize hydroxyl radicals after surface modification (Figures 7 and 8). By contrast, FA-PVA modified nanoparticles did not significantly produce hydroxyl radicals over time (Figure 8).

Discussion

Semiconductors have a wide variety of applications, ranging from microchips to solar cells. Recently, semiconductors have been used in implantable medical devices to monitor glucose levels in diabetics.[4] In this study, we go a step further by developing an injectable nanoscale semiconductor for potential use as a targeted cancer therapeutic. Specifically, we examine the properties of WO_3/Pt nanoparticles, which show promise for treating cancer via generation of cytotoxic ROS.

First, we optimized WO_3/Pt nanoparticles for ROS yield by examining the effect of crystal structure and platinization pH on ROS catalysis. WO_3/Pt nanoparticles exist as orthorhombic or tetragonal crystal structures, and the arrangement of atoms in the WO_3/Pt crystal lattice affects the availability of catalytic sites on WO_3/Pt surfaces. We found that orthorhombic WO_3/Pt nanoparticles exhibit higher ROS yields compared to tetragonal WO_3/Pt nanoparticles, suggesting that orthorhombic crystal structures allow for more oxygen vacancies which function as active sites for substrate binding (Figure 2). Moreover, we tested the effect of platinization pH on nanoparticle catalysis. Chloroplatinic acid was added to a suspension of WO_3 nanoparticles in pH 2, pH 12, and no buffer. WO_3 nanoparticles platinized at more basic pH have higher catalytic activity compared to WO_3 platinized at acidic pH. We believe that a basic pH destabilizes chloroplatinic acid, facilitating electron transport required for platinum deposition (Figure 3). Control WO_3 nanoparticles are poor photocatalysts due to the lack of platinum construct. Platinum helps trap electrons at the photocathode for the reduction of oxygen to hydroxyl radicals. We concluded that orthorhombic WO_3 nanoparticles platinized at basic pH are most suitable for use as experimental therapeutic photocatalysts. These nanoparticles were used in all subsequent studies.

After establishing a protocol for optimizing the ROS yield of WO_3/Pt nanoparticles, we studied the substrate specificity of WO_3/Pt. Our results show that WO_3/Pt nanoparticles extract

electrons from a wide variety of biomolecules to synthesize hydroxyl radicals. In particular, WO_3/Pt nanoparticles showed a high affinity for precursors to nucleic acids (uridine), amino acids (lysine, arginine), and metabolites (glucose, glycerol, oxalic acid, citric acid), suggesting that WO_3/Pt nanoparticles could interfere with key metabolic pathways including, but not limited to, the Krebs cycle, glycolysis, and protein synthesis (Figure 5). By sabotaging these vital metabolic pathways and destroying the constituents of tumor cells, WO_3/Pt nanoparticles could accelerate tumor cell failure. Moreover, WO_3/Pt nanoparticles have been shown to scavenge NADPH, a substrate for glutathione synthesis which participates in oxidant defense.[3] As such, WO_3/Pt nanoparticles not only produce ROS, but also weaken a tumor cell's ability to deflect an oxidant attack. Finally, the wide scope of biological substrates for WO_3/Pt nanoparticles provides an abundant supply of electrons for ROS synthesis. Therefore, we expect WO_3/Pt nanoparticles to be highly effective at inducing tumor cell apoptosis in vivo. These results were confirmed in animal studies, whereby injection of 4T1 cancer cells treated with WO_3/Pt nanoparticles into the anterior chamber of a mouse eye reduced tumor growth and extended lifetimes of mice.[3]

With confirmation that WO_3/Pt nanoparticles would be effective in vivo catalysts, we focused on developing a delivery platform to target WO_3/Pt nanoparticles to cancer cells while keeping them chemically active. Using CDI, we successfully coupled FA-PEG to the surface of WO_3/Pt nanoparticles, which was confirmed by both immunofluorescence and gel electrophoresis (Figure 6). As expected, FA-PEG coated nanoparticles migrated a shorter distance through the gel matrix than unmodified nanoparticles due to the hydrophobicity of the long carbon chain in FA-PEG, which reduces the overall surface charge of WO_3/Pt. Moreover, under microscope, modified nanoparticles stained with mouse anti folic acid antibody and Alexa Fluor 488 goat anti mouse antibody appeared fluorescent (Figure 4C). These data suggest that conjugation of FA-PEG to the surface of WO_3/Pt nanoparticles was successful.

After validating the linkage of FA-PEG to WO_3/Pt nanoparticles, we compared the catalytic activity of WO_3/Pt nanoparticles before and after surface modification using coumarin to track hydroxyl radical production. We found that surface modification of WO_3/Pt nanoparticles did not abolish catalytic activity. In fact, FA-PEG WO_3/Pt nanoparticles retained one half of their catalytic activity compared to control unmodified WO_3/Pt nanoparticles (Figure 7). Partial loss of activity could be due to the thick polymer coat of FA-PEG that blocks substrates from reaching the nanoparticle catalytic site, thus inhibiting hydroxyl production. However, when incubated with 4T1 cancer cells, FA-PEG WO_3/Pt nanoparticles did not bind specifically to cancer cells (data not shown).

To improve the tumor specificity of WO_3/Pt nanoparticles, we attempted to increase the density of FA on the surface of WO_3/Pt nanoparticles. We searched for polymers with a high content of amine functional groups, which are reaction sites for the covalent linkage of FA-NHS ester. Polyvinylamine (PVA) and poly-L-lysine (PLL) were used as linker molecules to increase the surface density of FA on WO_3/Pt nanoparticles (Figure 6A). FA was most abundant on FA-PVA modified WO_3/Pt nanoparticles (data not shown).

We compared the catalytic activity of FA-PVA and FA-PLL WO_3/Pt nanoparticles. We found that FA-PLL WO_3/Pt generated more hydroxyl radicals than FA-PVA WO_3/Pt, suggesting that FA-PLL would be more effective in vivo catalysts. Indeed, when tested in a model of breast cancer metastasis to the anterior chamber, FA-PLL nanoparticles selectively accumulated at tumors and induced tumor cell apoptosis under illumination.[10] Importantly, we demonstrated that targetable WO_3/Pt nanoparticles do not lose their ability to synthesize ROS after modification, and we optimized ROS yield and targeting efficiency by controlling both ligand type and surface density. Therefore, WO_3/Pt nanoparticles show promise for precise tumor treatment. By specifically localizing to nanometer sized regions in cancer cells, WO_3/Pt nanoparticles could locally manufacture ROS and spare healthy peripheral tissue from ROS-mediated damage.

Conventional ROS-based cancer such as radiotherapy and photodynamic therapy do not offer such specificity.

Remarkably, targetable WO_3/Pt nanoparticles could prove invaluable for eradicating cancer stem cells. Unlike other cells, cancer stem cells overexpress aldehyde dehydrogenase, an enzyme capable of detoxifying aldehydes which are produced via the lipid peroxidation pathway.[10] Although hydroxyl radicals generated by WO_3/Pt nanoparticles contribute to the lipid peroxidation pathway, aldehyde dehydrogenase enables cancer stem cells to resist nanoparticle treatment (Figure 9). However, combining WO_3/Pt nanoparticles with aldehyde dehydrogenase inhibitors could make cancer stem cells more vulnerable to treatment. Thus, by reducing cancer stem cell survival, WO_3/Pt nanoparticles could prevent tumor recurrence and eventually improve patient outcomes.

This work contributed to a recent publication in the scientific journal *Nanotechnology*.[3]

References

[1]Abe, Ryu, et al. "Pristine simple oxides as visible light driven photocatalysts: highly efficient decomposition of organic compounds over platinum-loaded tungsten oxide." Journal of the American Chemical Society 130.25 (2008): 7780-7781.

[2]Bonnett, Raymond, and Gabriel Martınez. "Photobleaching of sensitisers used in photodynamic therapy." Tetrahedron 57.47 (2001): 9513-9547.

[3]Clark, Andrea J., et al. "WO3/Pt nanoparticles are NADPH oxidase biomimetics that mimic effector cells in vitro and in vivo." Nanotechnology 27.6 (2015): 065101.

[4]Integrated Device Technology, Inc. “Implantable Glucose Sensor Featuring IDT Sensing Technology Awarded CE Mark.” *PR Newswire*. N.p., 22 June 2016. Web. 31 Mar. 2017.

[5]Kim, Jungwon, Chul Wee Lee, and Wonyong Choi. "Platinized WO3 as an environmental photocatalyst that generates OH radicals under visible light." Environmental science & technology 44.17 (2010): 6849-6854.

[6]Kim, Taeho, and Taeghwan Hyeon. "Applications of inorganic nanoparticles as therapeutic agents." Nanotechnology 25.1 (2013): 012001.

[7]Morales, Walter, et al. "Combustion synthesis and characterization of nanocrystalline WO3." Journal of the American Chemical Society 130.20 (2008): 6318-6319.

[8]Paciotti, Giulio F., David GI Kingston, and Lawrence Tamarkin. "Colloidal gold nanoparticles: a novel nanoparticle platform for developing multifunctional tumor-targeted drug delivery vectors." *Drug development research* 67.1 (2006): 47-54.

[9]Paszko, Edyta, et al. "Nanodrug applications in photodynamic therapy." Photodiagnosis and photodynamic therapy 8.1 (2011): 14-29.

[10]Petty, Howard, Dr. "A New Front in the War on Ocular Cancer." *The Ophthalmologist* 0217 (2017): 41-44. [9]Wicaksana, Yossy, et al. "Tungsten trioxide as a visible light photocatalyst for volatile organic carbon removal." Molecules 19.11 (2014): 17747-17762.

[11]Wen, Zhenhai, et al. "Ultrahigh-efficiency photocatalysts based on mesoporous Pt–WO 3 nanohybrids." Physical Chemistry Chemical Physics 15.18 (2013): 6773-6778.

Figures

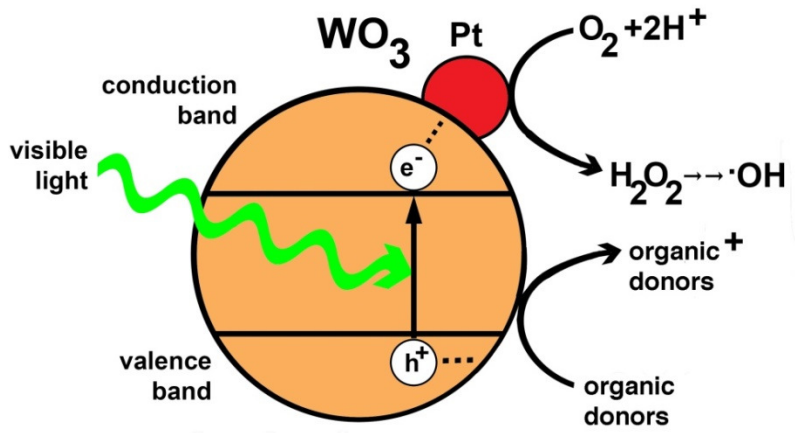

Figure 1. Photocatalytic reactions on WO_3/Pt nanoparticle surfaces
WO_3/Pt nanoparticles extract electrons from organic donors at the photoanode. Visible light excites electrons from the valence band to the conduction band where they are trapped by platinum and used to reduce oxygen into hydroxyl radicals at the photocathode.

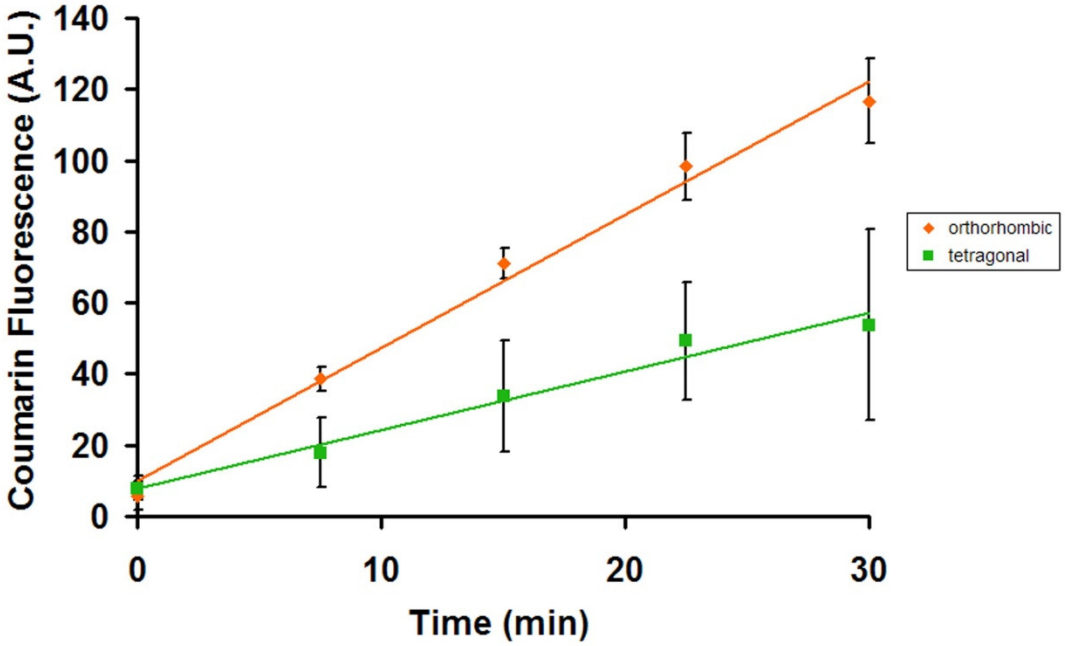

Figure 2. WO_3/Pt crystal structure affects ROS catalysis.
We evaluated the catalytic activity of different crystal structures of WO_3/Pt nanoparticles using coumarin as a fluorescent probe for hydroxyl radical production. A suspension of 0.5 mg/mL of WO_3/Pt nanoparticles in 1mM coumarin (pH 3) was illuminated for 30 minutes. Aliquots were sampled at five different time points and assessed for fluorescence (332/460). At 30 minutes, orthorhombic WO_3/Pt nanoparticles generate significantly more hydroxyl radicals than tetragonal WO_3/Pt nanoparticles ($n = 3$) ($p = 0.02$).

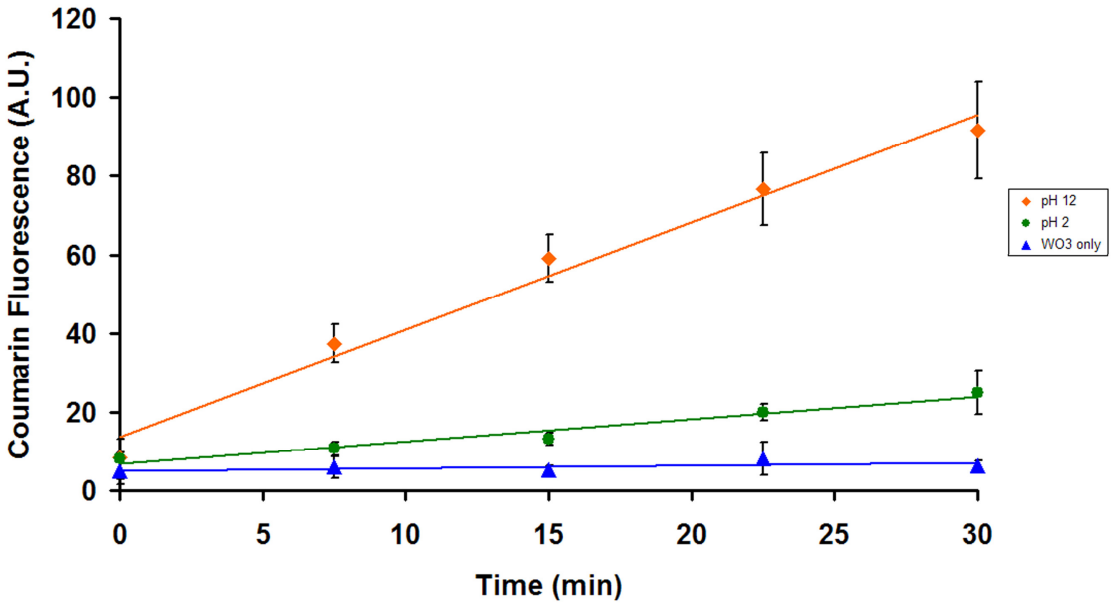

Figure 3. Platinization pH affects ROS catalysis.
We tested the effect of pH during platinum deposition on the catalytic activity of WO_3/Pt nanoparticles. Chloroplatinic acid was added to a suspension of WO_3 nanoparticles in pH 2, pH 12, and no buffer. Catalytic activity of resulting suspensions of WO_3/Pt nanoparticles was subsequently measured using a Coumarin assay. Platinum deposition at pH 12 resulted in significantly increased hydroxyl radical production compared to platinum deposition at pH 2 (n = 4) (p = 0.001).

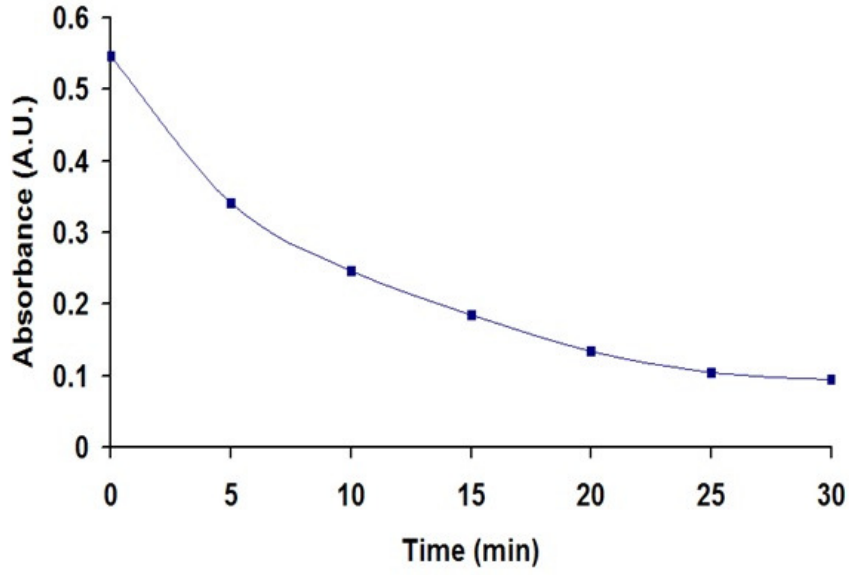

Figure 4. Degradation of Methylene Blue by WO_3/Pt nanoparticles
We monitored the degradation of methylene blue by WO_3/Pt nanoparticles over time using spectrophotometry. WO_3/Pt nanoparticles were added to a solution of methylene blue and illuminated with a visible light source. Methylene blue was degraded by WO_3/Pt over time. In the absence of light or nanoparticles, methylene blue was not degraded (data not shown).

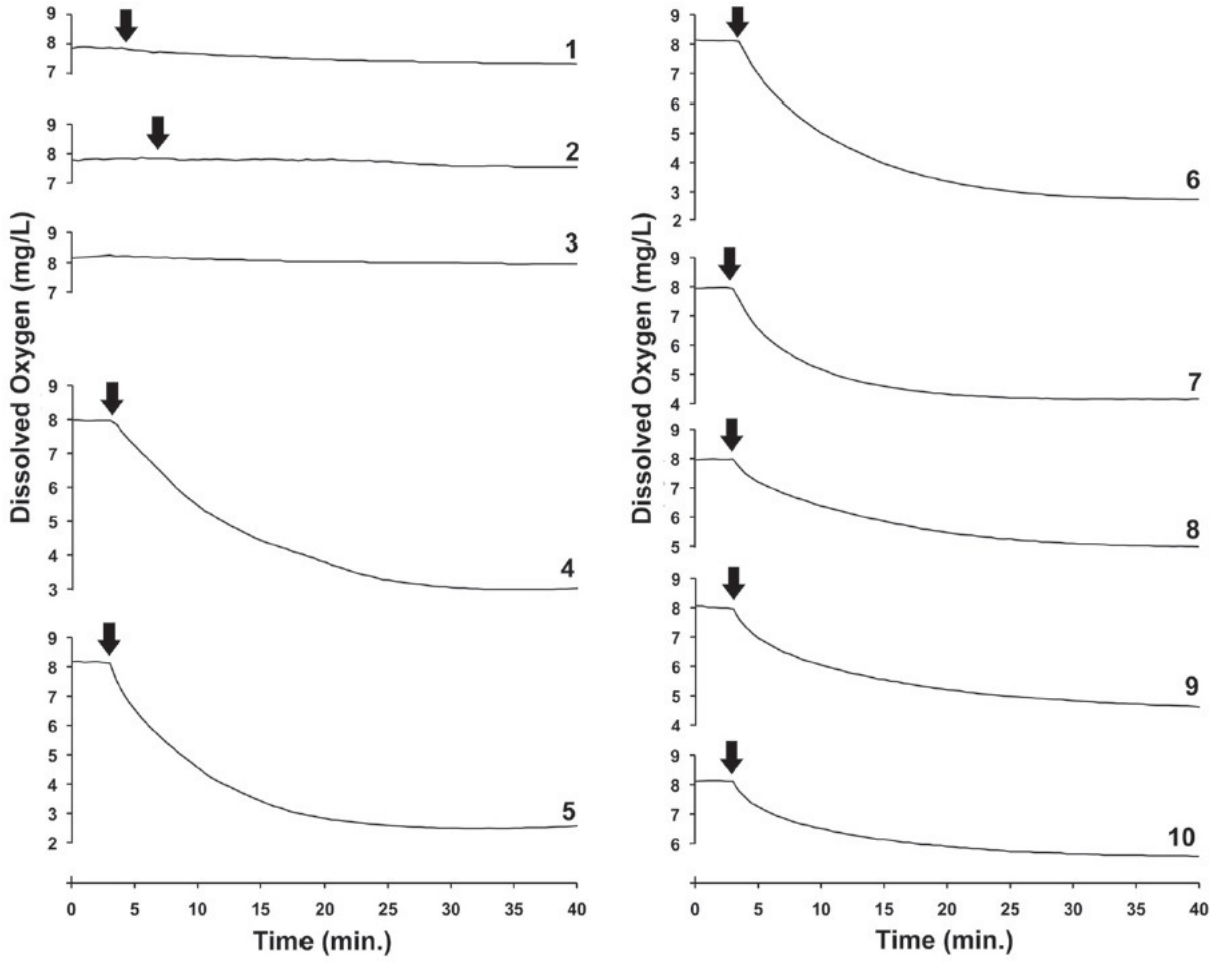

Figure 5. Substrate specificity of WO_3/Pt nanoparticles
We assessed the ability of a panel of biomolecules to act as substrates for WO_3/Pt nanoparticles in oxygen utilization experiments (n = 3). Arrows indicate the onset of illumination. Trace 1: A suspension of 1mg/mL of nanoparticles was illuminated in the absence of substrate. Trace 2: A 1 mM lysine solution was illuminated in the absence of nanoparticles. Trace 3: A mixture of nanoparticles and lysine was kept in the dark. Trace 4: Nanoparticles and lysine were exposed to light. Traces 5–10: Dissolved oxygen was measured in a suspension of nanoparticles and 1 mM arginine, 0.1% glucose, 0.1% glycerol, 0.1% citric acid, 0.1% oxalic acid and 1 mM uridine, respectively, during illumination. The combination of light, nanoparticles and substrate led to the disappearance of dissolved oxygen.

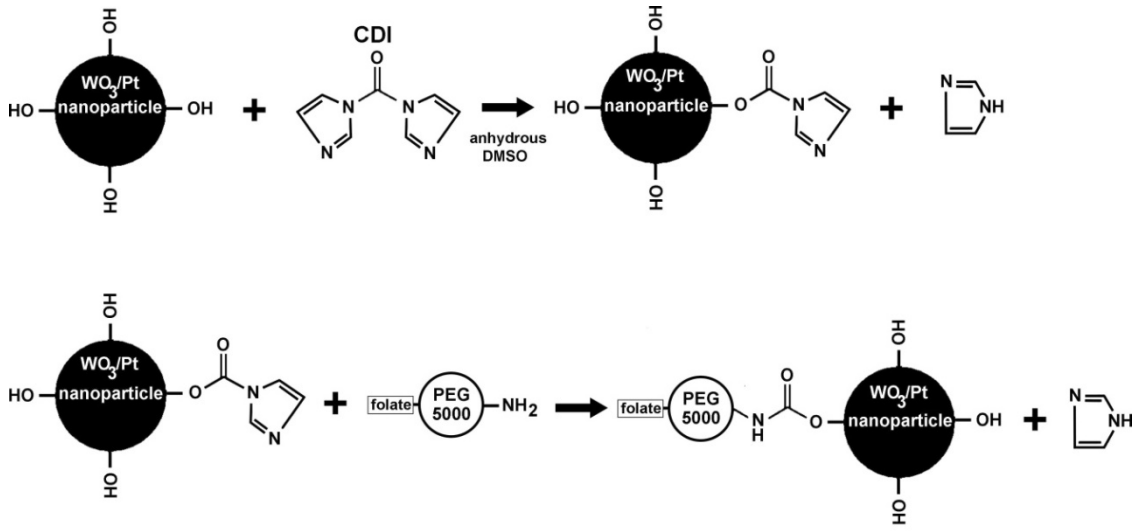

B)

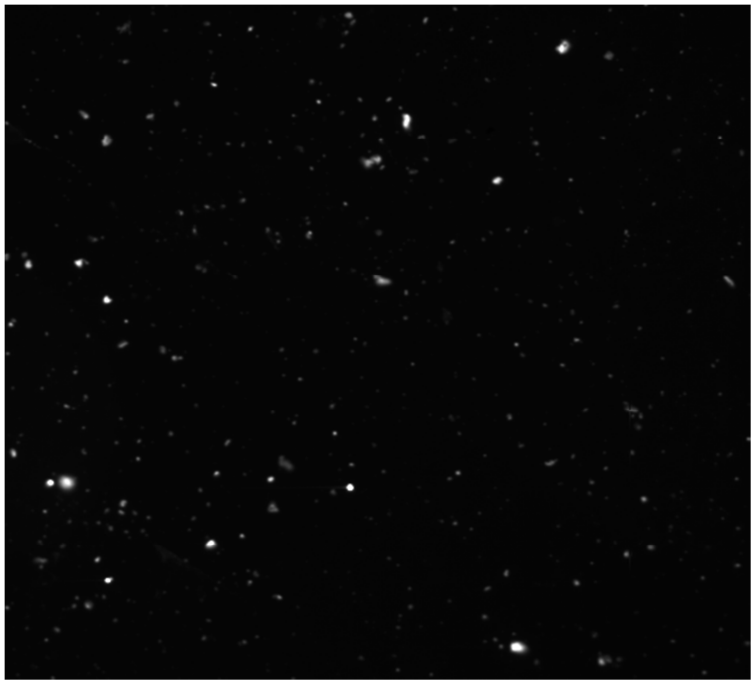

C)

Figure 6. Conjugation of FA-PEG to WO_3/Pt nanoparticles
A) Carbonyldiimidazole was used to covalently link FA-PEG to WO_3/Pt nanoparticles. First, nanoparticles were activated by CDI. Next, CDI-activated nanoparticles were reacted with FA-PEG amine overnight. B) We confirmed the linkage of FA-PEG to the surface of WO_3/Pt nanoparticles. Nanoparticles were successively stained with mouse anti folic acid antibody and Alexa Fluor 488 goat anti mouse antibody and visualized using immunofluorescence microscopy. C) Modified and unmodified nanoparticles were run in a 0.4% agarose gel at 60 mA. Lane 1: 25 µg of unmodified nanoparticles. Lane 2: 25 µg of FA-PEG nanoparticles.

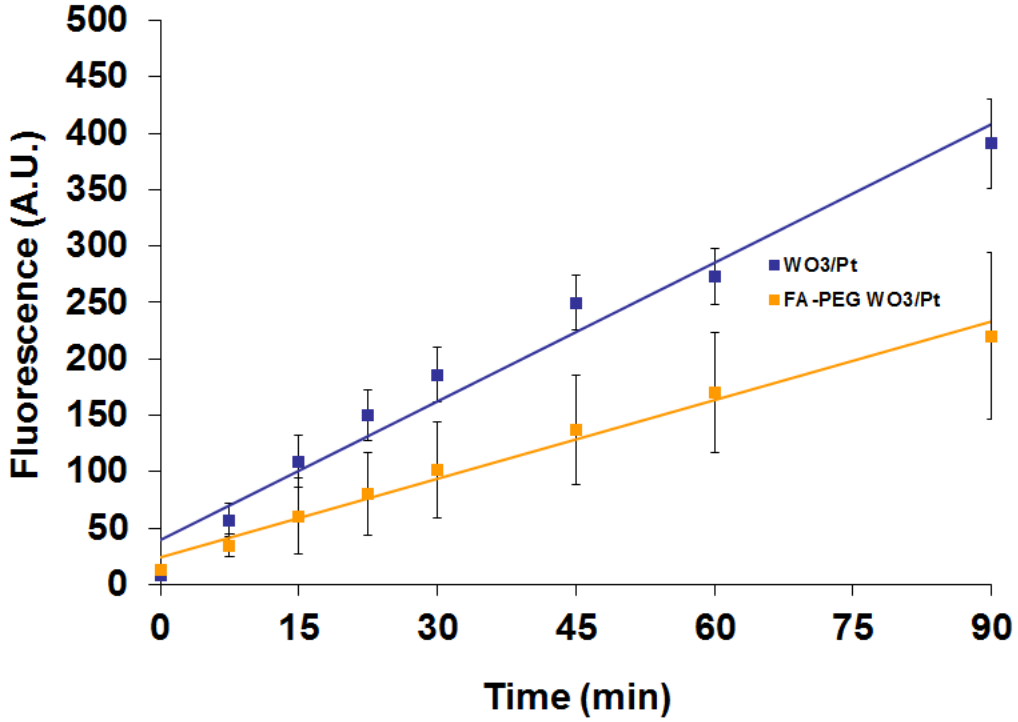

Figure 7. Photocathodic activity of FA-PEG WO_3/Pt nanoparticles
We monitored hydroxyl radical production at the photocathode using coumarin as a fluorescent probe. A suspension of 0.5 mg/mL of WO_3/Pt nanoparticles in 1mM coumarin (pH 3) was illuminated for 90 minutes (n = 3). Aliquots were sampled at eight different time points and assessed for fluorescence (332/460) using a fluorometer. The procedure was repeated after conjugation of FA-PEG to WO_3/Pt nanoparticles (n = 2). WO_3/Pt nanoparticles remained chemically active after surface modification.

A)

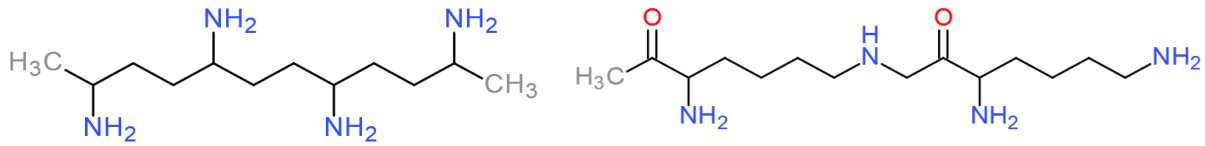

B)

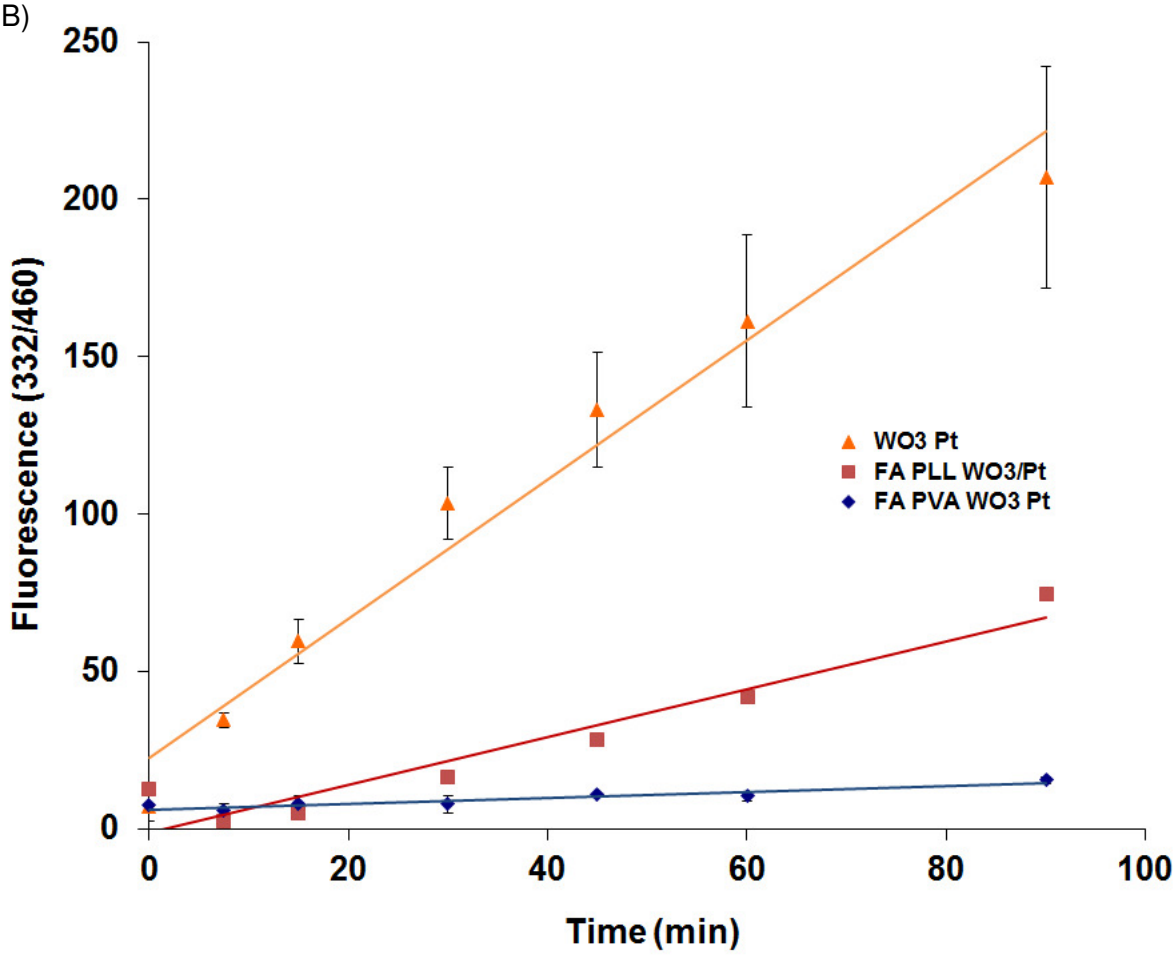

Figure 8. Photocathode activity of FA-PVA and FA-PLL nanoparticles
A) Polyvinylamine (left) offers the highest content of amine functional groups compared to poly-L-lysine (right). Amines are reaction sites for the conjugation of FA-NHS ester. Therefore, FA-PVA nanoparticles have a higher density of tumor targeting ligand FA. B) We assessed the photocathodic activity of modified and unmodified nanoparticles using a coumarin assay. A suspension of 0.5 mg/mL WO_3/Pt nanoparticles in 1mM Coumarin was illuminated for 90 minutes (n = 3). Aliquots were sampled at eight different time points and assessed for fluorescence (332/460) using a fluorometer. The procedure was repeated for FA-PVA WO_3/Pt (n = 3) and FA-PLL WO_3/Pt (n = 1). At 90 minutes, FA-PLL WO_3/Pt generated more hydroxyl radicals than FA-PVA WO_3/Pt.

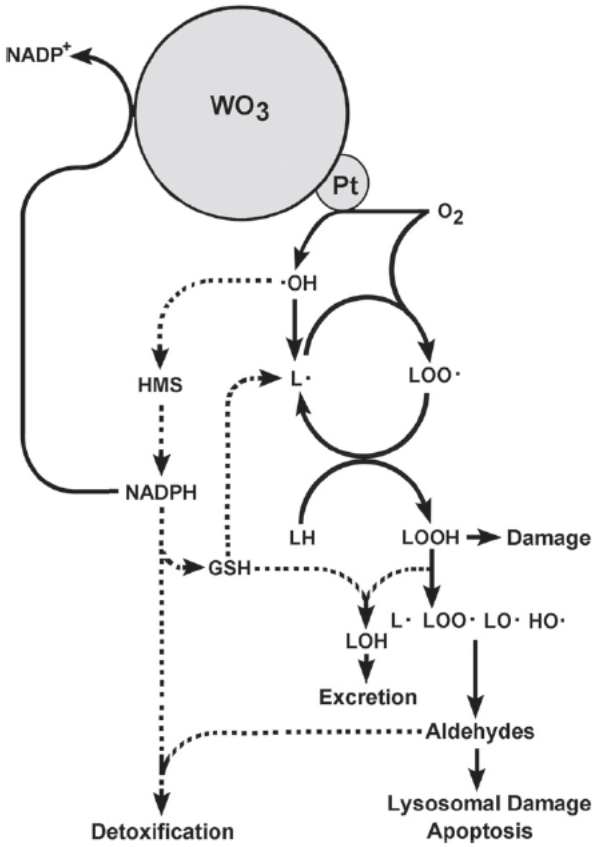

Figure 9. Biochemical pathways affected by WO_3/Pt nanoparticles
WO_3/Pt nanoparticles generate hydroxyl radicals from NADPH and other biological substrates. As a result, WO_3/Pt nanoparticles inhibit glutathione synthesis and reduce oxidant defense. Moreover, WO_3/Pt nanoparticles contribute to the lipid peroxidation pathway which produces toxic aldehydes (from Clark et al., 2015).